Vortex matter in $YBa_2Cu_3O_y$ single crystals investigated by scanning tunneling spectroscopy

Kenji Shibata,[1,*] Terukazu Nishizaki,[1] Makoto Maki,[2] and Norio Kobayashi[1,3]
[1]*Institute for Materials Research, Tohoku University, Sendai 980-8577, Japan*
[2]*Department of Physics, Saga University, Saga 840-8502, Japan*
[3]*Center for Low Temperature Science, Tohoku University, Sendai 980-8577, Japan*
(Received 16 May 2004; revised manuscript received 14 February 2005; published 14 July 2005)

To focus on the temperature and magnetic field dependence of the transformation of the vortex structure, systematic and direct investigations on the vortex configuration of $YBa_2Cu_3O_y$ (YBCO) have been performed by scanning tunneling spectroscopy at temperatures up to 90 K and magnetic fields up to 5 T. At low magnetic fields, we clearly observe a slightly distorted triangular lattice formed by vortices with sixfold coordination, which is attributed to the Bragg glass phase. This lattice transforms into a disordered structure in the presence of a high magnetic field. We observe that the disordered vortices form small clusters comprising fivefold and sevenfold coordination pairs. These microscopically determined vortex structures are in agreement with the vortex matter phase diagram derived from the macroscopic measurements, thus providing evidence of the field-driven disordering transition in the vortex solid phase of YBCO.

DOI: 10.1103/PhysRevB.72.014525 PACS number(s): 74.25.Qt, 74.72.Bk, 74.50.+r, 68.37.Ef

I. INTRODUCTION

The nature of the vortex solid phase in high temperature superconductors (HTSC) is influenced by various factors (such as $d_{x^2-y^2}$-wave effect, pinning effect, crystal structure anisotropy, intervortex interaction, thermal fluctuation, etc.), and this phase exhibits complicated behavior. This subject has attracted a considerable amount of attention and, as a consequence, numerous experimental and theoretical studies have been performed. Theoretical studies showed the vortex lattice structures on a magnetic field vs temperature plane of $d_{x^2-y^2}$-wave superconductors and suggested that the symmetry of the superconducting pair potential has a significant effect on that of the vortex system.[1,2] These studies have suggested that an increase in the magnetic field results in the transformation of the vortex lattice from a hexagonal into a square lattice. Experimentally, such a vortex lattice transformation was reported by the small angle neutron scattering (SANS) technique for $La_{1.83}Sr_{0.17}CuO_{4+\delta}$ (Ref. 3) and recently for $YBa_2Cu_3O_y$ (YBCO).[4]

However, real materials inevitably include a certain amount of disorder (e.g., impurities, atomic vacancies, twin boundaries, grain boundaries, etc.), which works as effective pinning centers for vortices and can affect the vortex lattice structure and alignment. Hence, in order to confirm the consistency between theoretical consideration and experimental results, it is important to investigate the effect of disorder. In high quality untwinned YBCO single crystals, the oxygen vacancies are the major sources for vortex pinning.[5] These vacancies are weak and random pointlike pinning centers. Giamarchi and Le Doussal proposed the concept of the Bragg glass phase, which, despite the existence of weak but finite pinning force, has quasi-long-range translational order without dislocations.[6] On the other hand, in strongly disordered samples, it was suggested that the low temperature phase is the vortex glass phase, which transforms into the liquid phase via the continuous second-order transition.[7,8] Moreover, for intermediate disorder, the presence of a multicritical point H_{mcp} was suggested on the liquid-solid phase transition line, where the first-order transition at low magnetic fields ends abruptly giving way to the continuous second-order transition at high magnetic fields at H_{mcp}. Thus, depending on the magnetic field strength, the vortex states at low temperatures are considered as the Bragg glass phase or the vortex glass phase. Experimental studies on overdoped YBCO (Refs. 9 and 10) as well as theoretical studies[6,11–13] suggested that the field-driven disordering transition line H^* is connected with H_{mcp} and divides the vortex solid phase into the Bragg glass phase and the vortex glass phase. It was also reported that a slight variation of the oxygen vacancies included in the sample have a significant influence on the H^* line.[14] However, direct evidence of the field-driven disordering transition in the vortex solid for YBCO has not yet been provided.

Recently, it has been theoretically suggested that the boundary between the hexagonal and the square vortex lattice exists in a magnetic field of ~1 T (Ref. 2) and ~6 T (Ref. 15) in YBCO. The magnetic field strength is comparable with the reported H^* line.[9,14] Experimentally, SANS results reported the transformation of the hexagonal vortex lattice into the square vortex lattice.[4] Thus, there is a conflict over the understanding of the vortex solid phase of YBCO in the presence of a high magnetic field. Direct, clear information for the vortex solid phase is an urgent requirement.

Scanning tunneling microscopy and spectroscopy (STM/STS) detects a local density of state which varies on the length scale of the coherence length ξ. STS is the only technique to visualize a local vortex configuration in real space in the presence of a high magnetic field of the order of a few Tesla. The pioneering STM/STS study on the vortex core states and the vortex configuration in YBCO was only performed at low temperature.[16] On the other hand, STM/STS studies of $Bi_2Sr_2CaCu_2O_{8+\delta}$ showed the presence of the disordered vortex structure at high magnetic fields.[17] However, systematic investigations on the temperature-magnetic field plane have not been performed using STM/STS on HTSC. This paper studies the structural transformation of the

vortex configuration in YBCO from a microscopic viewpoint, using the low temperature (LT) STM/STS. The vortex images are obtained at various temperatures and magnetic fields, and changes in the vortex structure are discussed. This study demonstrates the transformation of the vortex system from the ordered lattice state into the disordered state with changes in temperature and magnetic field strength.

II. EXPERIMENT

High quality YBCO single crystals were prepared by the self-flux method using Y_2O_3 crucibles. The samples used in this study showed a small number of twin boundaries of density less than 1 μm^{-2}. Slightly overdoped crystals ($T_c \sim 91$ K, $\Delta T_c \sim 1.5$ K) were prepared by annealing in an oxygen atmosphere of 1 bar at 450 °C. The annealed samples were chemically etched with 1% Br in ethanol for a minute, and subsequently rinsed in ethanol, followed by an immediate transfer into the loadlock chamber to be in a high vacuum. The surface prepared by the chemical etching process is quite stable and does not degrade by the exposure to an ultrahigh vacuum (UHV) up to room temperature, in contrast to the surface prepared by the low temperature cleaving process.[18] Thus, it implies that the topmost layer of the chemically etched sample is neither the highly reactive BaO layer nor the CuO-chain layer. We have as yet been unable to identify the topmost layer since we could not obtain atomic images of the chemically etched surface. The surface is quite flat and we observe only the step structures and twin boundaries on the surface.[19,20] Defects such as etch pits were not observed on the surface within our ~ 1 μm^2 scan range. The LT-STS apparatus used in this study was produced by UNISOKU Co, Ltd. and was partially improved by us. STS measurements were done at temperatures 4.5 K$\leqslant T \leqslant$90 K and magnetic fields up to 5 T (field cooled) parallel to the crystalline *c*-axis in UHV of 10^{-10} Torr. A mechanically sharpened Pt-Ir wire was used as the STM tip, which was approached perpendicular to the CuO_3 plane. The typical tunneling parameters for STS measurements are $V_{\text{sample}} = 0.03$ V and $I = 0.1$ nA for the set sample bias and the current, respectively, providing a tunneling resistance of 0.3 GΩ. Recently, we reported that the spectra inside and outside the vortex core regions show moderate differences at the bias voltage $|V_{\text{sample}}| \leqslant 25$ mV and cross at $|V_{\text{sample}}| \sim 10$ mV.[19,20] Therefore, in order to improve the signal-to-noise (S/N) ratio, all the vortex images in this paper were obtained by the following procedures. First, the I-V curves were measured typically at 128×128 points on a scan field. The differential conductance $dI(V)/dV$ was calculated for each I-V curve. The ratio of the integrated differential conductance in the vicinity of the coherence peaks to that at low energies was then calculated and mapped as follows: The $dI(V)/dV$ at energy ranging from -5 mV to 5 mV with 1 mV increments were calculated and added; $S(-5,5) = \Sigma_{V=-5}^{5} dI(V)/dV$. In a similar manner, $S(-25,-15) + S(15,25)$ was calculated and finally the ratio of $S(-25,-15)+S(15,25)$ to $S(-5,5)$ was mapped. The S/N ratio of the vortex imaging was improved by the method, and vortices were observed up to 80 K for our sample. The center of the scan area for each vortex image in this paper was confirmed to be at least 240 nm away from the twin boundary. Hence, the effect of the twin boundary on the vortex structure is expected to be negligible as reported in another study.[20]

III. RESULTS AND DISCUSSION

Figures 1(a)–1(e) show the vortex images taken at several temperatures at 1 T. In these figures, the directions of the crystalline axis are determined by the directions of the twin boundaries that are located far away from the displayed vortices.[20] Dark spots correspond to the vortex cores. In Fig. 1, the average density of the dark spots is approximately 5×10^{14} m^{-2}, which agrees with the calculated vortex density at 1 T. While vortices are successfully observed up to 80 K, a vortex image is not obtained at $T=90$ K. The spectrum at the vortex core at higher temperatures exhibits a very small difference from that at the superconducting region, making vortex imaging very difficult; this is one of the reasons that the vortex image is not obtained at 90 K. It can be supposed that the vortices at 90 K are in the vortex liquid phase and their movements make them invisible to STS. However at this point, we cannot ascertain the reason that the vortices are invisible at 90 K and 1 T, since we cannot provide evidence showing that the imaging contrast is preserved up to 90 K. Figures 1(f)–1(i) show the two-dimensional (2D) power spectra of the 2D Fourier transforms of the vortex images presented in Figs. 1(a)–1(d), respectively. The spots in each figure of Figs. 1(f)–1(i) exhibit a distorted hexagonal pattern at each temperature up to 80 K. This implies that within the measured areas, the vortices form the ordered lattice at 1 T.

The degree of disorder in a vortex configuration is also demonstrated by performing a Delaunay triangulation analysis to find the number of nearest neighbors (coordination number) for each vortex, which should be six for the perfect triangular lattice. The triangulation analysis directly demonstrates the position of disorder in the vortex lattices and the degree of topological disorder can be estimated by counting the number of disordered positions. The triangulation results of Figs. 1(a)–1(d) are shown in Figs. 1(j)–1(m), respectively. In these figures, the triangles correspond to the vortices with coordination number $z<6$, while the squares mark the vortices with $z>6$ (not shown in Fig. 1). The positions without these symbols show the vortices with coordination number $z=6$. It is clearly seen that the vortices with sixfold coordination are dominant, but at the same time, they are not perfectly aligned. A certain degree of vortex lattice distortion can be observed over the scan area. This implies that the vortex alignment is affected by the finite pinning force. As described earlier, the effect of the weak impurity or disorder on the vortex system is not negligible in HTSC; hence, such a slight distortion of the vortex lattice will be inevitable. Almost all the vortices exhibit sixfold coordination, despite the fact that they were slightly displaced. These results strongly suggest that the vortices are in the Bragg glass phase forming the distorted hexagonal lattice in this temperature and magnetic field region. Our results at 1 T are consistent with the results of Bitter decoration[21] and SANS

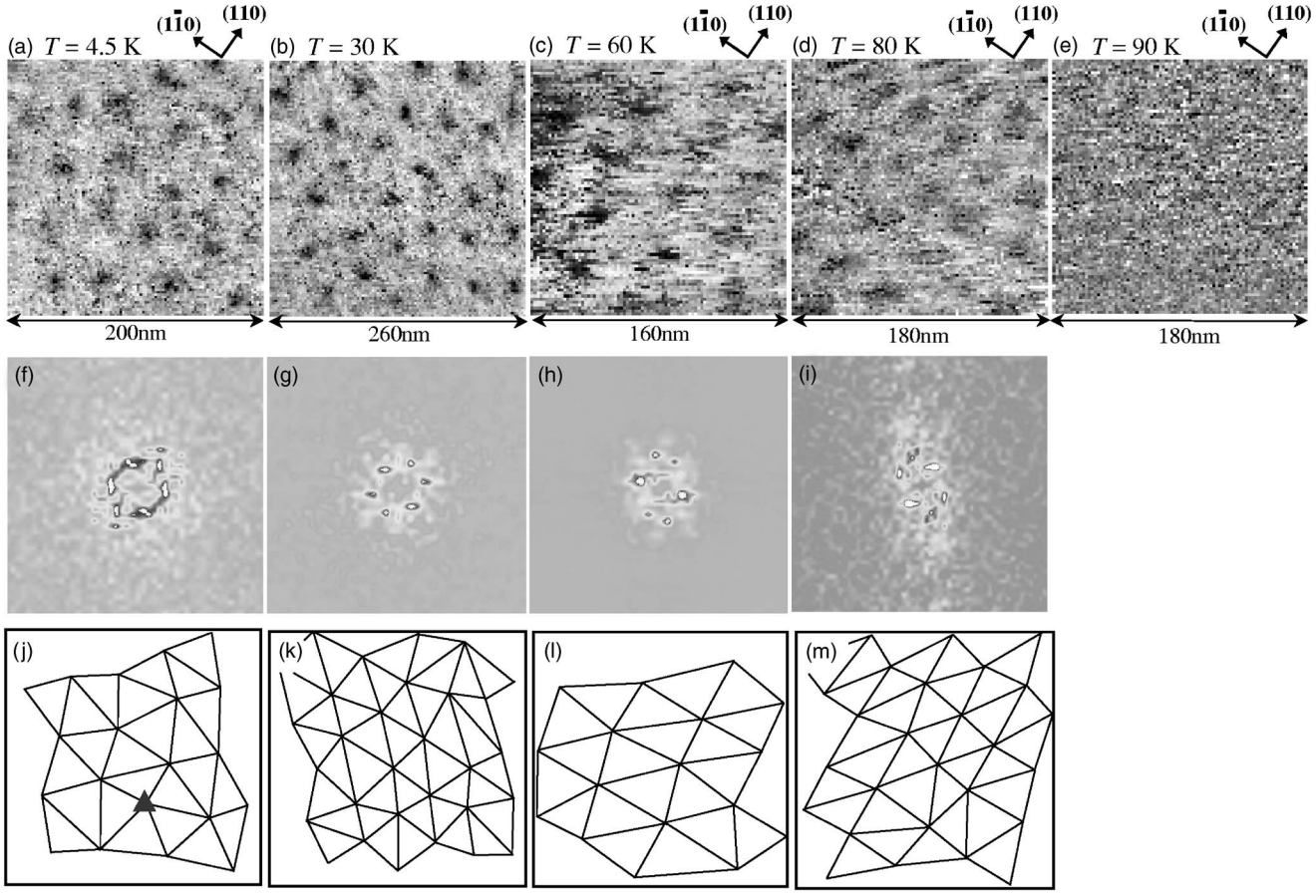

FIG. 1. STS images at temperatures (a) $T=4.5$ K, (b) $T=30$ K, (c) $T=60$ K, (d) $T=80$ K, and (e) $T=90$ K at magnetic field of 1 T. (f)–(i) represent the 2D power spectra of the vortex images shown in (a)–(d), respectively. (j)–(m) show the triangulation results of the vortex images shown in (a)–(d), respectively. In the case of the data at $T=30$ K, a twin boundary was not observed within ~ 1 μm^2 scan range; thus, the crystalline axis could not be determined.

measurements[4,22] at low temperature. Furthermore, our results demonstrate that vortices continue to form the distorted lattice state up to 80 K at 1 T. A fivefold coordination vortex can be seen only at 4.5 K [Fig. 1(j)], implying the presence of disorder in the vortex lattice. This observation is explained by the increase in the effective pinning force on vortices with decreasing temperature.

The symmetry of the superconducting order parameter becomes significant with an increasing magnetic field, since quasiparticle correlations between vortex cores become dominant. Thus, the vortex lattice aligns along the direction of the superconducting gap minimum, resulting in the formation of the square lattice.[1,2] At the same time, the effective disorder on the vortex system also increases with an increase in the magnetic field.[11] It causes disorder in the vortex lattice and the vortex system transforms into the disordered vortex glass phase. The systematic investigation of the vortex states in the presence of a higher magnetic field reveals anomalous and complicated vortex behavior.

Figure 2(a) shows a vortex image at 60 K and 3 T. The 2D power spectrum of Fig. 2(a) is shown in Fig. 2(b). Clear elongated spots are observed, suggesting the presence of the distorted hexagonal lattice rather than the square lattice. The orientation of the vortex lattice at 60 K and 3 T is slightly different from that at 60 K and 1 T [Fig. 1(h)]. Though the origin of the difference in the orientation is still open, it should be noted that the vortex lattice orientation and symmetry are expected to change gradually with an increase in the magnetic field.[1,2] Thus, our results at 60 K and 3 T appear to demonstrate that the vortices are on a process to transform from the hexagonal into square vortex lattice. The triangulation result of Fig. 2(a) is shown in Fig. 2(c). Only three among 29 vortices are detected to have fivefold or sevenfold coordination, implying that approximately 10% of the vortices have disordered configurations. The number of disordered vortices in the vortex system is slightly enhanced at 3 T as compared to that at 1 T.

Figure 2(d) shows a vortex image at 40 K and 3 T. From this figure, we extract several areas with the same scan size as that shown in Fig. 2(a), and the 2D power spectrum analysis is performed for each of these areas. One of the 2D power spectra for the extracted images is shown in Fig. 2(e). The 2D power spectrum exhibits an elliptical ringlike pattern and no more spots, indicating that the vortices form a disordered structure. The triangulation result of Fig. 2(d) is shown in Fig. 2(f). On the basis of the result, it can be observed that 38 among 83 vortices have fivefold or sevenfold coordination, implying that approximately 46% of the vortices have disordered configurations. This is very different from the results obtained at 60 K and 3 T (10% of the vortices are disor-

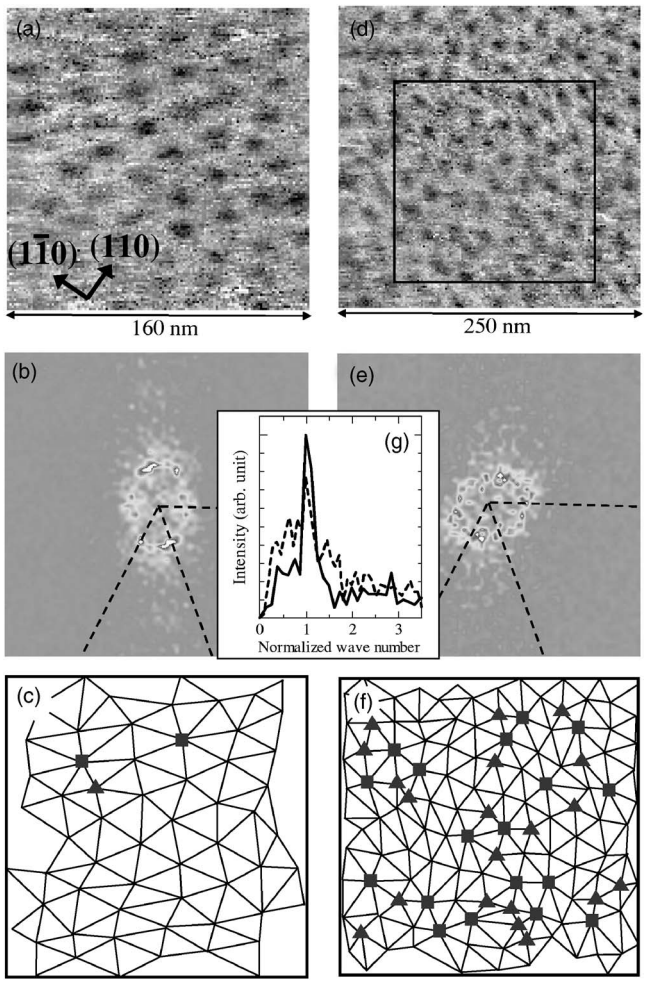

FIG. 2. (a) STS image (160×160 nm^2) at 60 K and 3 T. (b) 2D power spectrum of the vortex image of (a). (c) Triangulation result of (a). (d) STS image (250×250 nm^2) at 40 K and 3 T. (e) 2D power spectrum of the vortex image surrounded by the square (160×160 nm^2) in (d). (f) Triangulation result of (d). (g) The averaged cross sections of the power spectrum signals over the three radial directions represented as dashed lines in (b) and (e). The solid and dashed lines correspond to those in (b) and (e), respectively. The transverse values are normalized at the position at which the signal has the maximum value and then averaged.

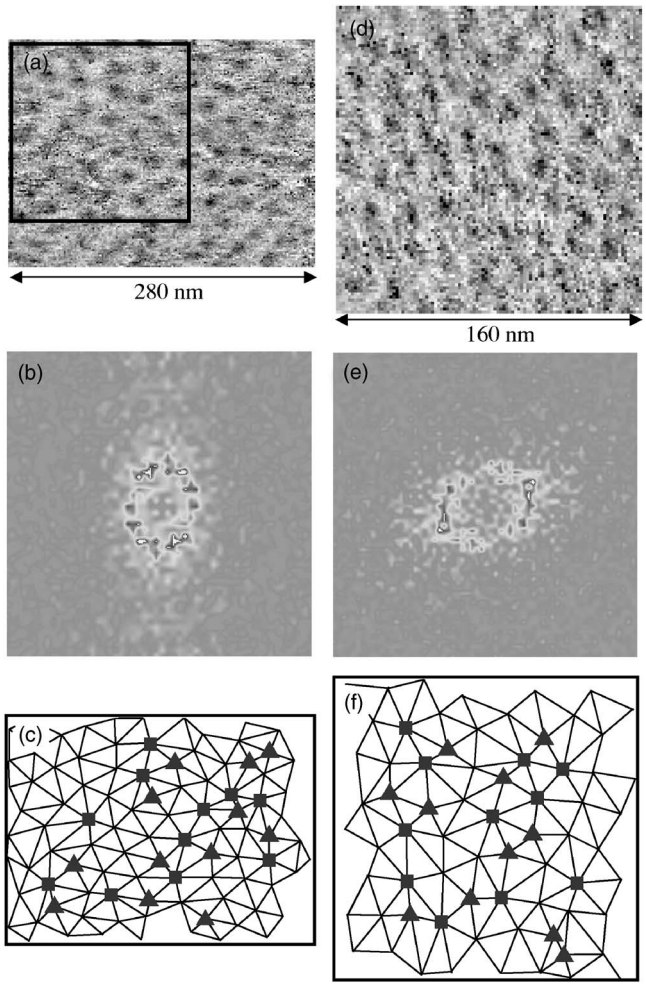

FIG. 3. (a) STS image (280×205 nm^2) at 4.5 K and 3 T. (b) 2D power spectrum of the vortex image surrounded by the square (160×160 nm^2) in (a). (c) Triangulation result of (a). (d) STS image (160×160 nm^2) at 4.5 K and 5 T. (e) 2D power spectrum of the vortex images shown in (d). (f) Triangulation result of (d).

dered). Power spectrum intensities at 3 T along the radial directions are also shown in Fig. 2(g) for 60 K (solid line) and 40 K (dashed line). The intensity at 40 K exhibits a broader and lower peak than that at 60 K, which indicates both the broader distribution in the intervortex distance and the suppression of the translational correlation. Thus, the temperature dependent enhancement of the disorder in the vortex system is clearly observed at 3 T. If we compare the triangulation results, we observe that the enhancement of the disorder at 3 T is very sharp between the vortex images for 60 K and 40 K. The origin of the disorder will be discussed later.

The vortex configuration is then shown in the presence of a higher magnetic field at 4.5 K. As shown in Fig. 1(a) (the vortex image), Fig. 1(f) (the 2D power spectrum), and Fig. 1(j) (the triangulation), the vortices form the distorted hexagonal lattice at 4.5 K and 1 T. Figure 3(a) shows a vortex image at 4.5 K and 3 T. While the vortices are clearly observed over the 280 nm$\times$205 nm scan area, subareas are extracted over a 160 nm$\times$160 nm scan area [e.g., the area surrounded by the square in Fig. 3(a)]; the 2D power spectrum is calculated, and shown in Fig. 3(b). The 2D power spectrum shows an elliptical ringlike pattern, indicating a disordered vortex configuration. Moreover, as shown in Fig. 3(c), the triangulation result demonstrates that 23 among 57 vortices (40%) have nonhexagonal coordination numbers. Figure 3(d) shows a vortex image at 4.5 K and 5 T. The 2D power spectrum and the triangulation result of Fig. 3(d) are also shown in Figs. 3(e) and 3(f), respectively. The triangulation result reveals that 22 among 36 vortices (61%) have disordered configurations. Moreover, it should be noted that the disordered vortices form small clusters, which are composed of almost the same number of vortices with fivefold and sevenfold coordination, as seen in Figs. 2(f), 3(c), 3(f). Since the disordered vortices form small clusters in the presence of a high magnetic field, the fraction of the disordered vortices depends on the specific area. More statistics are nec-

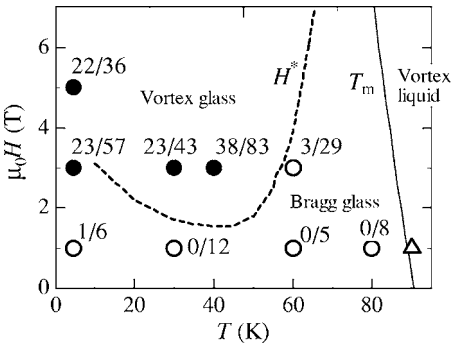

FIG. 4. Summary of the STS measurements on the structure of the vortex system. Measured points in the vortex solid phase are represented as circles on the *H-T* plane. Numbers near the circles denote the number of disordered vortices and the total number of vortices used in the triangulation analyses. The open and closed circles represent the positions at which the 2D power spectra of the vortex images show the distorted hexagonal spots and the ringlike pattern, respectively. The macroscopically determined melting transition line H_m and the field-driven disordering transition line H^* for the sample with the same oxygen content are also plotted in the form of solid and dashed lines, respectively. An open triangle indicates the position at which the STS measurement does not observe any vortex images.

essary to compare the number of disordered vortices at 3 T with that at 5 T. However, from the available statistics, it can be concluded that the vortices form highly disordered configurations at 4.5 K above 3 T.

The results of the 2D power spectra and the triangulation analyses are summarized in Fig. 4. In this figure, the circles represent the positions at which vortices are observed, and the numbers near the circles represent the number of disordered vortices and the number of vortices used in the triangulation analyses. The open and closed circles represent the positions at which the 2D power spectra of the vortex images exhibit distorted hexagonal spots and ringlike patterns, respectively. The vortex system at high temperatures and low magnetic fields clearly displays a relatively ordered configuration. On the other hand, at low temperatures and high magnetic fields, the vortices form disordered vortex structures. Our systematic investigations demonstrate microscopically this typical behavior of the vortex system.

In our STS measurements, the effect of the twin boundary on the local vortex configuration is negligible. Further, we have no evidence of surface defects such as etch pits. Thus, the only origin of the disorder is considered to be random point disorder such as oxygen deficiencies. The effect of random point disorder on the vortex phase diagram has been investigated intensively, and the presence of the field-driven disordering transition line H^* crossing the vortex solid phase has been suggested.[6,9–14] In Fig. 4, the macroscopically determined H^* line for the sample with the same oxygen content is represented by the dashed line.[9] The boundary between the ordered and the disordered region derived by the STS measurements agrees well with the H^* line, except at 4.5 K and 3 T. With an increase in the pinning force at low temperatures, the phase transition detected by the macroscopic methods (e.g., magnetization) becomes unclear, resulting in large errors in the H^* line (The errors below 30 K are estimated to be ±0.5 T, while they are estimated to be ±0.2 T at 60 K). We speculate that the vortex system at 4.5 K and 3 T is in the critical region between the Bragg glass phase and the vortex glass phase or just above the H^* line. Thus, our results confirm that the increase in the disorder of the vortex system in the presence of a high magnetic field is due to the field-driven disordering transition. According to Giamarchi and Le Doussal, dislocations, formed as vortex pairs with fivefold and sevenfold coordination, do not exist in the Bragg glass phase.[6] However, in actuality, a small number of dislocations are observed below the H^* line in the vortex images, as shown in Fig. 4. It should be noted that even in the Bragg glass phase, the pinning force will be enhanced at low temperatures or in the vicinity of the phase boundary to the vortex glass phase and will result in the generation of a small number of dislocations.

Recent SANS results for YBCO have reported the transformation of the hexagonal vortex lattice into the square lattice with increasing magnetic field up to $\mu_0 H = 11$ T.[4] This is apparently inconsistent with our results. However, it should be noted that a fully oxygenated sample with oxygen content $y \sim 7$ was used for the SANS measurement unlike the sample employed in this study ($y \sim 6.96$). We have reported that a marginal decrease in the oxygen concentration y from $y \sim 7$ to $y \sim 6.88$ leads to a drastic change in the vortex phase diagram.[14] In the fully oxygenated sample, the H^* line is expected to exist at $\mu_0 H^* \geqslant 10$ T; hence, it appears that the disordering transition does not occur in magnetic fields applied in the SANS measurement.[4] In the case of the slightly overdoped sample used in this study, the disordering transition line lies in the lower magnetic field of $1\ \mathrm{T} \leqslant \mu_0 H^* \leqslant 5$ T at low temperatures. Thus, the disordering transition of the vortex system can be observed in our study. However, since the vortex system forms the disordered state before it transforms into the square lattice, the transformation from the hexagonal to square lattice cannot be detected. In order to verify this, further experimental studies on samples with various oxygen deficiencies should be performed.

IV. CONCLUSION

We have performed scanning tunneling spectroscopy on the chemically etched surface of YBCO at various temperatures and magnetic fields. The vortex configuration in the vortex solid phase has been systematically investigated on the basis of the 2D power spectra and the triangulation analyses of STS images. The vortex solid phase is divided into two regions, the distorted hexagonal lattice state and the completely disordered state with a number of nonhexagonal coordination vortices. The structural transformation in the vortex solid phase is clearly detected in real space in YBCO for the first time in this study. It is also demonstrated that the microscopic vortex structures in the vortex solid phase agree well with those expected from the vortex matter phase diagram determined by the macroscopic measurements. Our results provide strong evidence for the presence of the field-driven disordering transition in the vortex solid phase of YBCO.

ACKNOWLEDGMENTS

The authors would like to thank T. Takahashi, S. Maekawa, Y. Iwasa, and T. Sasaki for valuable discussions. The authors are also grateful to M. Kawasaki and R. Takahashi for information on the surface preparation, as well as to T. Sasaki and T. Nagamura of UNISOKU Co., Ltd. for their technical support. This work was partly supported by a Grant-in-Aid for Scientific Research (Grant No. 15340107) from the Ministry of Education, Science, Sports, and Culture of Japan.

*Present address: Institute of Industrial Science, The University of Tokyo, 4-6-1 Komaba, Meguroku, Tokyo 153-8505, Japan.

[1] M. Ichioka, A. Hasegawa, and K. Machida, Phys. Rev. B **59**, 8902 (1999).

[2] J. Shiraishi, M. Kohmoto, and K. Maki, Phys. Rev. B **59**, 4497 (1999).

[3] R. Gilardi, J. Mesot, A. Drew, U. Divakar, S. L. Lee, E. M. Forgan, O. Zaharko, K. Conder, V. K. Aswal, C. D. Dewhurst, R. Cubitt, N. Momono, and M. Oda, Phys. Rev. Lett. **88**, 217003 (2002).

[4] S. P. Brown, D. Charalambous, E. C. Jones, E. M. Forgan, P. G. Kealey, A. Erb, and J. Kohlbrecher, Phys. Rev. Lett. **92**, 067004 (2004).

[5] M. Daeumling, J. M. Seuntjens, and D. C. Larbalestier, Nature (London) **346**, 6282 (1990).

[6] T. Giamarchi and P. Le Doussal, Phys. Rev. Lett. **72**, 1530 (1994); Phys. Rev. B **52**, 1242 (1995); **55**, 6577 (1997).

[7] M. P. A. Fisher, Phys. Rev. Lett. **62**, 1415 (1989).

[8] D. S. Fisher, M. P. A. Fisher, and D. A. Huse, Phys. Rev. B **43**, 130 (1991).

[9] T. Nishizaki, T. Naito, and N. Kobayashi, Phys. Rev. B **58**, 11169 (1998).

[10] K. Deligiannis, P. A. J. de Groot, M. Oussena, S. Pinfold, R. Langan, R. Gagnon, and L. Taillefer, Phys. Rev. Lett. **79**, 2121 (1997); H. Küpfer, Th. Wolf, C. Lessing, A. A. Zhukov, X. Lancon, R. Meier-Hirmer, W. Schauer, and H. Wuhl, Phys. Rev. B **58**, 2886 (1998); D. Giller, A. Shaulov, Y. Yeshurun, and J. Giapintzakis, *ibid.* **60**, 106 (1999); S. Kokkaliaris, P. A. J. de Groot, S. N. Gordeev, A. A. Zhukov, R. Gagnon, and L. Taillefer, Phys. Rev. Lett. **82**, 5116 (1999).

[11] D. Ertas and D. R. Nelson, Physica C **272**, 79 (1996).

[12] J. Kierfeld, Physica C **300**, 171 (1998).

[13] D. Carpentier, P. L. Doussal, and T. Giamarchi, Europhys. Lett. **35**, 379 (1996); J. Kierfeld, T. Nattermann, and T. Hwa, Phys. Rev. B **55**, 626 (1997); D. S. Fisher, Phys. Rev. Lett. **78**, 1964 (1997); V. Vinokur, B. Khaykovich, E. Zeldov, M. Konczykowski, R. A. Doyle, and P. H. Kes, Physica C **295**, 209 (1998).

[14] K. Shibata, T. Nishizaki, T. Sasaki, and N. Kobayashi, Phys. Rev. B **66**, 214518 (2002).

[15] B. Rosenstein and A. Knigavko, Phys. Rev. Lett. **83**, 844 (1999).

[16] I. Maggio-Aprile, Ch. Renner, A. Erb, E. Walker, and O. Fischer, Phys. Rev. Lett. **75**, 2754 (1995).

[17] Ch. Renner, B. Revaz, K. Kadowaki, I. Maggio-Aprile, and O. Fischer Phys. Rev. Lett. **80**, 3606 (1998); S. H. Pan, E. W. Hudson, A. K. Gupta, K.-W. Ng, H. Eisaki, S. Uchida, and J. C. Davis, *ibid.* **85**, 1536 (2000); B. W. Hoogenboom, K. Kadowaki, B. Revaz, M. Li, Ch. Renner, and O. Fischer, *ibid.* **87**, 267001 (2001); K. Matsuba, H. Sakata, N. Kosugi, H. Nishimori, and N. Nishida, J. Phys. Soc. Jpn. **72**, 2153 (2003).

[18] M. Maki, T. Nishizaki, K. Shibata, T. Sasaki, and N. Kobayashi, J. Phys. Soc. Jpn. **70**, 1877 (2001); M. Maki, T. Nishizaki, K. Shibata, and N. Kobayashi, Phys. Rev. B **65**, 140511(R) (2002).

[19] K. Shibata, M. Maki, T. Nishizaki, and N. Kobayashi, Physica C **388-389**, 277 (2003).

[20] K. Shibata, M. Maki, T. Nishizaki, and N. Kobayashi, Physica C **392-396**, 323 (2003).

[21] P. L. Gammel, D. J. Bishop, G. J. Dolan, J. R. Kwo, C. A. Murray, L. F. Schneemeyer, and J. V. Waszczak, Phys. Rev. Lett. **59**, 2592 (1987); G. J. Dolan, F. Holtzberg, C. Feild, and T. R. Dinger, *ibid.* **62**, 2184 (1989).

[22] S. T. Johnson, E. M. Forgan, S. H. Lloyd, C. M. Aegerter, S. L. Lee, R. Cubitt, P. G. Kealey, C. Ager, S. Tajima, A. Rykov, and D. McK. Paul, Phys. Rev. Lett. **82**, 2792 (1999).